

**Effect of Maturity and Mineralogy on Fluid-Rock Reactions in
the Marcellus Shale**

Journal:	<i>Environmental Science: Processes & Impacts</i>
Manuscript ID	EM-ART-09-2018-000452.R2
Article Type:	Paper
Date Submitted by the Author:	30-Jan-2019
Complete List of Authors:	Pilewski, John; West Virginia University, Geology and Geography Sharma, Shikha; West Virginia University, Geology and Geography Agrawal, Vikas; West Virginia University, Geology and Geography Hakala, J.; National Energy Technology Laboratory, U.S. Department of Energy Stuckman, Mengling; National Energy Technology Laboratory, U.S. Department of Energy

Environmental Significance Statement

Natural gas exploitation from the Appalachian Basin has significantly increased in the past decade. The push to properly dispose, reuse, or recycle the large amounts of produced fluid associated with hydraulic fracturing operations and designing better fracturing fluids has necessitated a better understanding of the subsurface chemical reactions taking place during hydrocarbon extraction. This study reports results of laboratory experiments conducted to understand the effect of varying maturity and mineralogy of shale on the proliferation of inorganic ions and low molecular weight organic compounds, mainly benzene, toluene, ethylene, and xylene (BTEX) and monosubstituted carboxylic acids in the reservoir after injection of hydraulic fracturing fluids.

Effect of Maturity and Mineralogy on Fluid-Rock Reactions in the Marcellus Shale

John Pilewski¹, Shikha Sharma^{1}, Vikas Agrawal¹, Alexandra Hakala², Mengling Y. Stuckman²*

¹ West Virginia University Department of Geology & Geography, 330 Brooks Hall, 98 Beechurst Ave. Morgantown, WV 26506

² National Energy Technology Laboratory, U.S. Department of Energy, Pittsburgh, PA 15236

*Corresponding Author : E-mail: shikha.sharma@mail.wvu.edu Phone: 304-293-6717

ABSTRACT

Natural gas exploitation from the Appalachian Basin has significantly increased in the past decade. The push to properly dispose, reuse, or recycle the large amounts of produced fluid associated with hydraulic fracturing operations and designing better fracturing fluids has necessitated a better understanding of the subsurface chemical reactions taking place during hydrocarbon extraction. Using autoclave reactors, this study mimics conditions of deep subsurface shale reservoirs to observe the chemical evolution of fluids during the shut-in phase of hydraulic fracturing (HF), a period when hydraulic fracturing fluid (HFF) remains closed in the reservoir. The experiment was conducted by combining synthetic hydraulic fracturing fluid and powdered shale core samples in high temperature/pressure static autoclave reactors for 14 days. Shale samples of varying maturity and mineralogy were used to assess the effect of these variations on the proliferation of inorganic ions and low molecular weight volatile organic compounds (VOCs), mainly benzene, toluene, ethylbenzene and xylenes (BTEX) and monosubstituted carboxylic

1
2
3 acids. Ion chromatography results indicate the relative abundance of ions present were similar to
4 those of produced water from HF operations in the Marcellus Shale basin. There was an increase
5 of SO_4^{2-} and PO_4^{3-} and the decrease in Ba^{2+} upon fluid-shale reaction. Major ionic shifts indicate
6 calcite dissolution in two of the fluid-shale reactions and barite precipitation in all fluid-shale
7 reactions. Toluene, xylene, and carboxylic acids were produced in the shale-free control
8 experiment. The most substantial increase in BTEX analytes was observed in reactions with low
9 maturity shale, while the high maturity shale reaction produced no measurable BTEX compounds.
10 Total organic carbon decreased in all reactions including fracturing fluid and shale, suggesting
11 adsorption onto the organic matter (OM) matrix. The results from this study highlight that both
12 the nature of OM and mineralogy play a key role in determining the fate of inorganic and organic
13 compounds during fluid-shale interactions in the subsurface shale host rock. Overall this study
14 aims to contribute to the growing understanding of complex chemical interactions that occur in the
15 shale reservoirs during HF, which is vital for determining potential environmental impacts of HF
16 and designing more efficient HFF and produced water recycling techniques for environmentally
17 conscious natural gas production.
18
19
20
21
22
23
24
25
26
27
28
29
30
31
32
33
34
35
36
37
38

39 **1.0 Introduction**

40
41 The Marcellus Shale is the largest natural gas producing reservoir in the United States, and over
42 the past decade, the amount of natural gas extracted from the reservoir has almost tripled due to
43 advancements in horizontal drilling technologies.¹ As a result, thousands of wells have been
44 drilled in areas of Pennsylvania, Ohio and West Virginia, where most of the reservoir is
45 underlain. Hydraulic fracturing is applied to stimulate production from tight reservoirs and
46 involves the injection of millions of gallons of fluid (hydraulic fracturing fluid, HFF), which is
47 comprised of water, sand, and chemical additives.^{2,3} Injected HFF is known to react with the
48
49
50
51
52
53
54
55
56
57
58
59
60

1
2
3 reservoir rocks, resulting in changes in reservoir porosity and permeability due to HFF-mineral
4 interactions.⁴⁻⁷ These reactions also affect the chemistry of fluids produced from the
5 formation.^{8,9} Therefore, these interactions can affect both long-term hydrocarbon productivity
6
7 from shale reservoirs and produced fluid treatment and management strategies. One area of study
8 that requires further investigation is understanding the effect of HFF-shale reactions on the
9 potential release of organic constituents, such as BTEX compounds, into fluids produced from
10 the reservoir. Knowledge of how shale thermal maturity, and transformation of HFF additives
11 under reservoir conditions, affect the composition of produced fluids is needed to improve the
12 efficiency of fracturing treatments and the efficacy of produced fluid management. The overall
13 outcome would be a reduced environmental footprint for hydrocarbon production from
14 unconventional reservoirs.
15
16
17
18
19
20
21
22
23
24
25
26
27
28
29

30 The composition of produced fluids from both active wells and laboratory-based
31 experiments differed from initial injection fluid in prior studies, indicating that reservoir
32 reactions and fluid mixing may both contribute significantly to produced water chemical
33 signatures.⁸⁻¹¹ Produced water from unconventional reservoirs is typically characterized by its
34 relatively high total dissolved solids (TDS), varying concentrations of dissolved organic carbon
35 (DOC), and sometimes an abundance of radioactive elements.^{4,12,13} Monocyclic aromatic
36 hydrocarbons such as benzene, toluene, ethylbenzene, xylene, and low molecular weight organic
37 acids represent common soluble organic compounds observed in produced water.^{3,14-16}
38
39 Determining the source of soluble organic compounds is particularly challenging due to
40 variations in organic additives used from well to well and the difference in organic matter
41 throughout different maturity zones of the Marcellus Shale.¹⁷ Identifying sources of organic
42 carbon and its evolution throughout the HF process is crucial for predicting which additives to
43
44
45
46
47
48
49
50
51
52
53
54
55
56
57
58
59
60

1
2
3 use in HFF and how it can be handled at the surface after it has interacted with the organic-rich
4 shale in the reservoir.
5
6

7
8
9 Hydraulic fracturing fluid (HFF) is comprised of three main ingredients: 95% fresh
10 water, 4% proppant or silica sand, and 1% chemical additives by wt%.¹⁸ Although chemical
11 additives constitute only 1% of the total fluid injected, at volumes of 3-4 million gallons of
12 injected fluid per well (e.g., per disclosures reported in FracFocus), this can result in 30,000 to
13 40,000 gallons of injected chemical additive. In the initial stages of fracturing, the friction of
14 HFF must be lowered via friction reducing organic additives such as WFR-61LA,² which
15 contains petroleum distillates and ethoxylated alcohols. Gelling agents are included in order to
16 increase the HFF viscosity to transport proppant into the induced fractures, which produce a
17 linked 3D polymer structure with the addition of cross linkers such as boric acid and
18 ethanolamine. Breaker compounds, such as ammonium persulfate, are included in the HFF
19 mixture to subsequently react with the proppant transport gel to reduce the HFF viscosity for
20 flowback. The breaker compounds are often included with the overall HFF mixture. However,
21 these are expected to become reactive after a period of time, or under certain reservoir
22 conditions. For example, ammonium persulfate creates SO_4^{2-} free radical ions to break down the
23 gel at elevated temperatures above 50°C.^{15,16,19}
24
25
26
27
28
29
30
31
32
33
34
35
36
37
38
39
40
41
42
43
44

45 The Marcellus Shale is characterized by its low permeability and high concentrations of total
46 organic carbon (TOC).¹ The reservoir varies in depth longitudinally, increasing from 3,000 ft in
47 the northwest to 8,000 ft in the southeastern portion of the reservoir. This variation in depth
48 results in different maturity windows throughout the reservoir ranging from 0.5% R_o (percentage
49 of vitrinite reflectance) at shallower depths up to 3.5% R_o at the deepest zones of the reservoir.¹
50
51
52
53
54
55
56
57
58
59
60

1
2
3 Gas-rich, over mature zones of the Marcellus, contain type II-III kerogen that has been thermally
4 altered, providing a predominantly aromatic chemical signature.²⁰⁻²³ Less mature zones have
5 similar type II-III kerogen, but it has not been thermally degraded or altered to the same extent,
6 resulting in a relatively more aliphatic chemical signature.^{21,24} It is possible that the shallow, less
7 mature zones of the Marcellus Shale contain aliphatic chemical structures that serve as the source
8 of labile organic compounds released during the well shut-in period.
9

10
11 Variations in shale mineralogy also may affect the reactivity of both organic additives in the
12 HFF and the shale kerogen. The Marcellus Shale is comprised of mostly mixed-layer clays,
13 quartz, feldspar, calcite, and pyrite.¹ Relative abundances of these minerals can vary from zone
14 to zone and can control the system's buffering capacity and alteration of organic material.
15 Previous fluid-rock reaction studies conducted at ambient pressures showed that the mineralogy
16 of the shale, especially calcite and pyrite content, control the precipitation of iron-bearing
17 minerals, removal/release of metal contaminants, the evolution of fluid composition and porosity
18 destruction or development.^{5,6} Calcite rich shales possess high pH buffering capacity, which
19 favors pyrite dissolution, the release and oxidation of Fe²⁺ ion and formation of Fe (III)- bearing
20 precipitates.^{5,6} These studies also show that calcite and pyrite dissolution can cause a release in
21 metal contaminants whereas Fe-(oxy)hydroxide precipitation leads to removal of metal
22 contaminants from solution. A recent study²⁵ shows that fracturing fluid interactions can also
23 lead to significant changes in carbonyl content, aromaticity, average aliphatic chain length and
24 release of metals from kerogen isolates. Although these studies provide a preliminary
25 understanding of inorganic and organic reactions that might take place during shale-fracturing
26 fluid interactions, they were performed at ambient pressure conditions as opposed to in situ
27 reservoir pressure conditions.
28
29
30
31
32
33
34
35
36
37
38
39
40
41
42
43
44
45
46
47
48
49
50
51
52
53
54
55
56
57
58
59
60

1
2
3 The objective of this study is to perform laboratory experiments to effectively simulate fluid-
4 shale reactions under in situ, high pressure/temperature reservoir conditions, and to elucidate the
5 fate of inorganic and organic reactants and products from HF operations within different
6 maturity zones of a reservoir. To our knowledge, this is one of the first study that has tried to
7 compare shale-fluid interactions in shale samples collected across a range of maturity from a
8 single shale basin. Determining the downhole chemical evolution of the fluid used to fracture the
9 Marcellus Shale is critical for improving hydrocarbon recovery from tight shales and identifying
10 effective water treatment and management strategies for produced fluids.
11
12
13
14
15
16
17
18
19
20
21
22

23 **2.0 Materials and Methods**

24
25
26 Fluid-shale reactions were conducted using Parr 4768 static autoclaves to mimic and analyze
27 the in situ fluid-shale reactions during the shut-in phase of hydraulic fracturing. The specific
28 analyses focused on the major changes of inorganic ions and the proliferation of low molecular
29 weight organic compounds within the fluid.
30
31
32
33
34
35

36 ***2.1 Sampling and Preparation***

37
38
39
40 The fluid used in the reaction vessels was a mixture of synthetic formation brine and
41 synthetic HFF, prepared per methods reported for core flood experiments simulating the shut-in
42 period for a Marcellus Shale HF operation, as reported⁴ (Table 1). The three shale samples of
43 varying maturity were collected from Marcellus Shale cores from different depths and
44 geographical zones of the reservoir (Table 2). All samples have TOC values greater than 9 wt%,
45 and OM sourced from mixed marine and terrestrial sources, representing type II-III kerogen.
46
47
48
49
50
51
52

53
54 ^{20,21,26} The maturity of the samples is represented as a percent vitrinite reflectance (%R_o). The %
55
56
57
58
59
60

1
2
3 R_0 is calculated directly from the T_{max} , a thermal maturity parameter determined by pyrolysis
4 analysis, and is the temperature where the hydrocarbon generation rate from kerogen peaks.²⁷
5
6

7 Mineralogy was analyzed as part of this study (Table 2) and is further described in both the
8 methods and results sections. To prepare shale samples for the static autoclave reactions, core
9 samples were first washed using deionized water to avoid contamination from drill mud, then
10 crushed using SPEX mixer mill to 100 mesh powder to maximize surface area and enhance
11 reaction kinetics.
12
13
14
15
16
17
18
19

20 ***2.2 Experimental Design***

21
22
23

24 To emulate reservoir conditions during the shut-in phase, experiments were conducted
25 using two 4768 Parr Instrument Company 600-ml high-temperature/pressure vessels set to
26 ~2,500 psi and 100°C respectively. These values were used to best mimic in situ reservoir
27 conditions of the Marcellus Shale while remaining within the limitations of the vessels.^{4,8} Inside
28 each 600-ml pressure vessel, a small Teflon cup was placed containing a fixed HFF-shale ratio
29 (20:1) of 400 mL of fluid and 20 g of shale, following a previous study.⁸ The remaining volume
30 of each vessel was then filled with pressurized, inert N_2 (100% pure) to 2,500 psi. Four
31 experiments were conducted, each for 14 days to mimic an intermediate-term shut-in phase of an
32 HF operation⁴. One experiment only contained HFF (no shale), and the other three experiments
33 were performed with both HFF and the three shale samples described above. Fluids and shale
34 were mixed immediately prior to pressurizing the reactors. Duplicate experiments were not
35 performed due to limitations in the availability of shale samples.
36
37
38
39
40
41
42
43
44
45
46
47
48
49
50
51
52
53
54
55
56
57
58
59
60

2.3 Analytical Methods

Five fluid samples were collected and analyzed in this study: NR-HFF (Non-Reacted Hydraulic Fracturing Fluid: the original fracturing fluid synthesized for this study) that served as control, HPT-HFF (High Pressure/Temperature Hydraulic Fracturing Fluid; HFF exposed to high pressure and temperature in the absence of shale), and LM-2, WV-7, and MIP-3H fluids collected after the fluid-shale reactions with respective shale samples.

Fluid samples were collected from the reactors at the conclusion of the 14-day experiment using a high-density polyethylene Luer syringe and filtered via a 0.45 μ m WhatmanTM syringe filter attachment. Samples for ion chromatography (IC, ThermoFisher ICS-5000+ with AS11-HC column for anion and CS16 column for cation quantification) were collected with minimal headspace in 10 mL plastic vials. The IC analysis focused on observing low molecular weight mono substituted carboxylic acids (e.g., acetate, formate, butyrate, and succinate) and dissolved major cations and anions of interest in this study (e.g., Ba²⁺, SO₄²⁻, and PO₄³⁻). All the samples were run in triplicates, and the standard error of IC measurements reported here were generally less than \pm 3%. Additionally, every 10-20 samples, a cation/anion control sample (Sigma Aldrich, Inc.) was added during measurements, whose accuracy is within 95% - 105%. The detection limit of the organic acids and ions analyzed in this study are indicated in Table 3 and Table 4.

Sample splits for non-purgeable organic carbon (NPOC) and dissolved inorganic carbon (DIC) were analyzed with a Shimadzu Total Organic Carbon/Total Inorganic Carbon (TOC/TIC) Analyzer. Average values from 3-5 replicates were reported with < 2% precision (%RSD), and

1
2
3 quality control samples for every 10-12 samples demonstrated consistent accuracy within 95%-
4
5 105%.
6
7

8
9 Volatile organic carbon (VOC) analytes were sampled in accordance with methods described
10
11 in Chapter 4 of *EPA SW-486 Compendium: Organic Analytes*. Samples for VOC analysis were
12
13 placed in pre-cleaned 60 mL volatile organic analysis (VOA) vials and acidified with minimal
14
15 headspace to preserve target analytes. VOCs were efficiently transferred from the aqueous phase
16
17 to the vapor phase by bubbling helium at a flow rate of 40mL/min through a portion of the
18
19 aqueous sample at ambient temperature and purged for 11 minutes. The vapor is swept through
20
21 a sorbent trap (Supelco Trap A, Tenax 24cm) where the volatile components are adsorbed. The
22
23 sorbent trap is then heated at 180°C for 12 minutes and backflushed with an inert gas to desorb
24
25 the components onto a gas chromatographic (GC) column (30m x 0.53mmID VOCOL capillary
26
27 column with 3µm film thickness). A temperature program of 2°C/min to 75°C (with initial
28
29 temperature 45°C) then to 25°C/min to 220°C and hold 2 minutes was used in the gas
30
31 chromatograph (GC) to separate the organic compounds. Detection is achieved by a photo-
32
33 ionization detector (PID) for detection of the aromatic compounds. This analysis was performed
34
35 at REIC Labs in Morgantown, WV, within one day of sampling and kept at 4°C until analyzed.
36
37 The analysis was conducted in accordance with EPA Method 8260B and analytes of focus
38
39 included benzene, toluene, ethylbenzene and xylene with a detection limit of 1 µg/ml for
40
41 benzene, toluene, ethylbenzene, and o-xylene and 2 µg/ml for m/p xylene.
42
43
44
45
46
47
48

49 Mineral compositional analysis was performed on powdered shale samples (using SPEX
50
51 mixer mill), using a PANalytical X'Pert Pro X-ray Diffractometer with a CuKα source at 2θ
52
53 angles from 5° to 75° and a step time of ~12 s per degree (total scan time 13.5 min). 20-mm slit
54
55
56
57
58
59
60

1
2
3 was used to focus X-rays onto an Xcelerator™ detector. Samples were irradiated on a spinning
4 stage (1 revolution/s), with antiscatter and divergence slit angles of 1° and 0.5°, respectively. The
5 x-ray beam was operated at current 40 mA and voltage 45 kV. Spectra were interpreted using the
6 X'pert HighScore Plus Program to evaluate the percentage of various mineral phases present.
7
8 Semi-quantitative estimation of percentages was performed using the reference-intensity ratio
9 (RIR) matrix-flushing method^{28,29} based on selected PDF2 reference samples chosen for each
10 mineral phase. The minerals wt % were calculated to the nearest unit, and the total sum of the
11 minerals was within 100 ± 1 wt %.

12
13
14
15
16
17
18
19
20
21
22
23 Geochemical modeling of the IC and DIC data for each fluid (NR-HFF, HPT-HFF, LM-2,
24 WV-7, and MIP-3H), was performed using Geochemists Workbench Professional v. 10.0 using
25 the MINTEQ database to calculate saturation indices for minerals in the system (sulfate,
26 carbonate, and phosphate bearing).

3.0 Results

3.1 Mineralogy and Aqueous Inorganic Chemistry

31
32
33
34
35
36
37
38
39
40 The Marcellus Shale samples in this study were mixed layer clays with lower fractions of
41 carbonate, quartz, pyrite, and feldspar as compared to clay minerals (Table 2), consistent with
42 mineral compositions in previous studies.^{30,31} Calcite abundance differed amongst the samples,
43 in which it was identified in the LM-2 (21 wt%) and MIP-3H (16 wt%) samples, however, it was
44 not detected in the WV-7 sample (Figure 1). Dolomite and pyrite were both detected within 1 –
45 10 wt% in all three shale samples (dolomite: LM-2 5 wt%, WV-7 4 wt%, and MIP-3H 5 wt%;
46
47
48
49
50
51
52
53
54
55
56
57
58
59
60 pyrite: LM-2 and MIP-3H 5 wt%, and WV-7 2 wt%). Mixed clay and quartz content varied

1
2
3 amongst all samples (Table 2). No direct relationship was observed between mineralogy and
4 thermal maturity (Figure 1). However TOC decreased with increasing thermal maturity (Table
5
6
7
8
9
10
11
12
13
14
15
16
17
18
19
20
21
22
23
24
25
26
27
28
29
30
31
32
33
34
35
36
37
38
39
40
41
42
43
44
45
46
47
48
49
50
51
52
53
54
55
56
57
58
59
60

amongst all samples (Table 2). No direct relationship was observed between mineralogy and thermal maturity (Figure 1). However TOC decreased with increasing thermal maturity (Table 2).

Results indicate that except sulfate, almost all cations and anions are reduced by half on increasing pressure and temperature in shale-free fracturing fluids (HPT-HFF) as compared to initial non reacted NR-HFF (Table 3). However, the most measurable changes observed in IC-analyzed inorganic species are for shale-reacted fluids, where both SO_4^{2-} and PO_4^{3-} increased and Ba^{2+} decreased (Table 3, Figure 2). Sulfate concentrations in the shale-reacted samples were all elevated relative to the HPT-HFF sample, which is the shale-free control experiment (Table 3, Figure 2). The NR-HFF and HPT-HFF shale-free samples contained 9.6 mg/L SO_4^{2-} and 10.6 mg/L SO_4^{2-} , respectively. For experiments containing shale, SO_4^{2-} was 189.8 mg/L (LM-2), 271.5 mg/L SO_4^{2-} (WV-7), and 66.1 SO_4^{2-} (MIP-3H). Barium concentrations in the shale-reacted samples were either substantially lower (less by at least 70%), or non-detectable, relative to the shale-free control sample HPT-HFF (Table 3, Figure 2). All shale-reacted samples showed a substantial decrease in Ba^{2+} relative to the shale-free experiments ($[\text{Ba}^{2+}] = 3.8$ mg/L (LM-2), 10.6 mg/L Ba^{2+} (MIP-3H), and not-detectable (WV-7)), while the shale-free samples contained $[\text{Ba}^{2+}] = 96.2$ mg/L (NR-HFF), and 39.1 mg/L (HPT-HFF). No measurable PO_4^{3-} was present in NR-HFF or HPT-PF, however it was detected in all shale-reacted fluids ($[\text{PO}_4^{3-}] = 6.9$ mg/L (LM-2), 29.8 mg/L PO_4^{3-} (WV-7), and 9.6 mg/L (MIP-3H)) (Table 3, Figure 2). The pH values in shale-free conditions remained low, where NR-HFF was 1.3 and HPT-HFF was 1.9. For the shale-reacted samples, pH values varied and were measured as 2.3 (WV-7), 5.73 (MIP-3H), and 6.07 (LM-2) (Table 3). Dissolved inorganic carbon was detected in only two samples, LM-2 and

1
2
3 MIP-3H. LM-2 contained 35.18 C mg/L DIC and MIP-3H contained 15.8 mg/L DIC. WV-7
4
5 fluid had no observable inorganic carbon (Table 3).
6
7

8 9 ***3.2 Aqueous Organic Chemistry***

10
11
12 Substantial changes in the organic chemistry of fluids from all experiments performed at
13
14 elevated pressure and temperature were observed relative to the shale-free control that remained
15
16 at ambient conditions. Target volatile organic compounds (VOCs) were detected in the shale-free
17
18 HPT-HFF sample (no shale, elevated P,T), which also contained elevated non-purgeable organic
19
20 carbon (NPOC) relative to the control NR-HFF fluid (no shale, ambient P,T) (Table 4). For
21
22 experiments with shales of different thermal maturity, VOCs were detected at higher
23
24 concentrations in the low-maturity shale (LM-2) relative to all other samples, and at around the
25
26 same levels for the intermediate-maturity shale (WV-7) as the HPT-HFF sample. VOCs were not
27
28 detected in fluids from the experiment with the highest thermal maturity shale (MIP-3H) (Table
29
30
31 4, Figure 3A).
32
33
34
35

36
37 The target VOC analytes, BTEX compounds, were observed in HPT-HFF at relatively low
38
39 concentrations. HPT-HFF fluid contained toluene concentrations of 2.7 $\mu\text{g/L}$ and xylene
40
41 concentrations of 9.7 $\mu\text{g/L}$. Fluid from the LM-2 reaction was the only sample which contained
42
43 benzene, at a concentration of 2.5 $\mu\text{g/L}$. The LM-2 sample also contained toluene (14.8 $\mu\text{g/L}$)
44
45 and xylene (15.8 $\mu\text{g/L}$). The WV-7 fluid contained toluene (1.3 $\mu\text{g/L}$) and xylene (7.1 $\mu\text{g/L}$).
46
47 HPT-HFF, WV-7 and LM-2 samples no measurable amount of ethylbenzene, fluid from the
48
49 MIP-3H reaction produced no observable BTEX compounds. It is also important to note that
50
51 NR-HFF had no measurable BTEX compounds (Table 4, Figure 3A).
52
53
54
55
56
57
58
59
60

1
2
3 No direct trend between fluid-phase NPOC and either the R_0 or the experimental P and T,
4 were observed (Table 4). The NPOC values were elevated in some experiments performed at
5 elevated P,T (HPT-HFF > LM-2) relative to the shale-free ambient P,T fracturing fluid (NR-
6 HFF), however, two experiments contained lower NPOC (NR-HFF > MIP-3H > WV-7) (Table
7 4). Low molecular weight organic acids (acetate, formate, butyrate, and succinate) were detected
8 in all experimental fluids, and they were the highest in the HPT-HFF and lowest in NR-HFF
9 (Table 4, Figure 3B). Fluids from the experiments containing shale contained different
10 proportions of individual organic acids; however, the total values were similar across the three
11 shale samples, and individual organic acids did not display any trends with thermal maturity
12 (Table 4, Figure 3B).
13
14
15
16
17
18
19
20
21
22
23
24
25

26 27 **4.0 Discussion**

28 29 30 ***4.1 Inorganic Mineral Reactions affecting Shale Composition and Produced Fluid Chemistry***

31
32
33
34 Changes in the inorganic fluid chemistry amongst the five experimental fluids demonstrate
35 that inorganic reactions occur both due to changes from ambient to elevated P,T, conditions, and
36 during interaction between HFF and the shale. A net decrease (almost half) in almost all cations
37 (Na^+ , K^+ , Ba^{2+} , Sr^{2+} , Mg^{2+} , and Ca^{2+}) upon increasing pressure and temperature of the shale-free
38 HFF sample occurred (compare NR-HFF and HPT-HFF in Table 3). The observed change in
39 inorganic ions (especially cations) could result from chelation with fracturing fluid additives, or
40 potential chemical transformation or precipitation during the experiment. Chelation of inorganic
41 ions is possible due to the presence of ligands in scaling inhibitors and cross linkers (such as
42 ethylene glycol or ethanolamine) in the fracturing fluid. For example, ethylene glycol is reported
43 to form complexes with certain divalent metal halides.³² Additionally, if anions such as Br^-
44
45
46
47
48
49
50
51
52
53
54
55
56
57
58
59
60

1
2
3 transformed to BrO_3^- due to reaction with sulfate radicals,³³ present as a result of ammonium
4 persulfate breakdown in our experiments, the resulting BrO_3^- anion would not be detectable with
5 the IC method applied in this study. Changes in temperature also may have resulted in the
6 formation of non-detected precipitates in the reactor, or that were removed during fluid sampling
7 and filtration.³⁴ Geochemical modeling was used to understand the evolution of inorganic species
8 in the experiments. However, the changes observed in the IC analysis between NR-HFF and
9 HPT-HFF are not consistent with the predictions of the model (Table. 5). This could be because
10 geochemical modeling software does not account for the effect of processes like chelation and
11 filtration on the fluid chemistry. Although the interaction of HFF with the wall of the reactor
12 could occur, this is unlikely as the containers used to conduct the experiments were made of
13 Teflon, which is not anticipated to affect the cationic composition of the fluids. There is a
14 possibility of adsorption/desorption of organic molecules on the Teflon. However, the
15 experimental conditions for all the reactions (with and without shale) were same. Therefore,
16 relative differences observed in the concentration of organic molecules between different
17 experiments are most likely due to shale fracturing fluid interactions.

18
19
20
21
22
23
24
25
26
27
28
29
30
31
32
33
34
35
36
37
38
39 Reactions involving shale appear to be largely controlled by reactions involving carbonate
40 minerals. The HFF formulation applied in this study included HCl and started with low pH
41 (Table 1, Table 3), which is common for HFF applied in the Marcellus Shale.⁶ HCl is used for
42 cleaning perforations prior to injecting fracturing fluid mixtures and is a common additive used
43 to prevent scaling of secondary minerals.¹⁸ The pH in our LM-2 and MIP-3H fluid samples rose
44 substantially (to 6.1 and 5.7, respectively; Table 3), indicating that carbonate minerals in these
45 shale samples acted as effective buffers during the reaction similar to prior observations.^{4,5,8,35}
46
47
48
49
50
51
52
53
54
55 The pH in our WV-7 sample remained low, with a similar value to the HPT-HFF (no-shale)
56
57
58
59
60

1
2
3 experiment at elevated P, T, indicating the minimal buffering capacity of the WV-7 shale (Table
4
5 3).

6
7
8
9 Differences between the pH buffering capacity between the LM-2, MIP-3H, and WV-7
10 samples can be explained through differences in calcite content between the samples, where LM-
11 2 and MIP-3H contain 21 and 16 wt%, respectively, while calcite was not detected in WV-7
12 (Table 2, Figure 1). Calcite saturation indices calculated for our experimental fluids (only LM-2
13 and MIP-3H, as these were the only samples with detectable DIC as a calculation input), showed
14 that both shale-reacted solutions were undersaturated with respect to calcite (Table 5). These
15 results are consistent with other studies focused on HFF-shale reactions, which showed that
16 calcite content of the shale significantly controlled pH buffering and mineral dissolution and
17 precipitation reactions.^{4-6,8,35}

18
19
20
21
22
23
24
25
26
27
28
29
30
31 The potential for mineral scale formation involving barite was evaluated for our experiments,
32 based on the changes in Ba^{2+} and SO_4^{2-} observed between the experiments with and without
33 shale (Table 3, Figure 2). Application of the experimental data towards geochemical equilibrium
34 calculations showed that barite is supersaturated in all experimental fluids, except for the WV-7
35 experiment (Table 5). The only reason for this difference with WV-7 is because no Ba^{2+} was
36 detected via IC for the fluid sample, which likely indicates that all Ba^{2+} in that experiment was
37 removed via precipitation. Barite precipitation during HFF-shale interaction has been observed
38 by various investigators,^{4,7,36} has the potential to affect shale porosity and permeability,^{4,7} and
39 may play a role in shale oxidation-reduction.^{8,37}

40
41
42
43
44
45
46
47
48
49
50
51
52
53 Multiple sources for Ba^{2+} and SO_4^{2-} exist in the HFF-shale reaction scenario. Although Ba^{2+}
54 in unconventional reservoirs may originate from trapped drilling muds,³⁸ Ba^{2+} also may be
55
56
57
58
59
60

1
2
3 present within the shale, release upon HFF-shale interaction under low pH conditions, and re-
4 precipitate once carbonate mineral dissolution buffers the system pH.^{7,9,37,38} Potential sources of
5 SO_4^{2-} include fracturing fluid additives (e.g., ammonium persulfate), sulfate-bearing minerals in
6 the shale (e.g., anhydrite), and oxidative dissolution of pyrite.^{5,8,39} Previous studies postulate that
7 due to the high buffering capacity of calcite, shale samples containing a higher content of calcite
8 result in the higher dissolution of pyrite and higher concentration SO_4^{2-} .^{5,6}
9
10
11
12
13
14
15
16
17

18 In our study, it was observed that the WV-7 shale sample had the highest SO_4^{2-} concentration
19 even though it contains the least amount of calcite and pyrite as compared to LM-2 and MIP-3H
20 shale samples (Table 3, figure 2). This is in contrast to conclusions made by previous studies.^{5,6}
21 We postulate that a large amount of sulfate formation in the WV-7- fracturing fluid experiments
22 results from the more extensive breakdown of the ammonium persulfate breaker. This could
23 possibly result from the presence of higher clay content (almost twice) in WV-7 sample. Clay
24 carries a net negative charge on its surface which can interact with the ammonium ion (NH_4^+) in
25 the ammonium persulfate breaker. We postulate that association of NH_4^+ with negatively
26 charged clay surfaces could enhance dissociation of ammonium persulfate. Higher breakdown of
27 ammonium persulfate will release more sulfate ions into the solution. The higher sulfate
28 concentration will also lead to the formation of higher amount BaSO_4 precipitate by taking up
29 free barium ions present in the solution. We postulate that this ultimately results in a greater
30 decrease in barium ions in WV-7 reacted fluid sample as compared to LM-2 and MIP-3H reacted
31 fluid samples (Fig. 2, Table 3).
32
33
34
35
36
37
38
39
40
41
42
43
44
45
46
47
48
49
50

51 A new observation from the experiments performed with this study is the change in fluoride and
52 phosphate concentrations in fluids from certain HFF-shale experiments, and the subsequent
53
54
55
56
57
58
59
60

1
2
3 supersaturation of certain PO_4^{3-} and F-bearing minerals (Tables 3 and 5). The absence of PO_4^{3-}
4
5 in the NR-HFF and HPT-HFF, and increase in concentrations in all fluid samples, is evidence
6
7 that the F and PO_4^{3-} is leaching from the powdered shale (Table 3). The possible sources of F
8
9 and PO_4^{3-} are from apatite ($\text{Ca}_5(\text{PO}_4)_3(\text{OH})$, $\text{Ca}_{10}(\text{PO}_4)_5(\text{CO}_3)\text{F}_3$) and fluorite minerals present
10
11 in shale samples (Table. 5). Although, these phases were not detected in XRD analysis probably
12
13 because of their lower abundance in the samples, but a prior study on Marcellus shale also
14
15 detected evidence for authigenic apatite minerals such as carbonate fluorapatite using a
16
17 phosphate-specific sequential extraction step.⁴⁰ The variations in concentrations of F and PO_4^{3-}
18
19 in the fluid samples could possibly be due to the variations in concentrations of the F and PO_4^{3-}
20
21 rich minerals in the shale and/or different eh and pH conditions of the solution. The higher
22
23 concentration of F and PO_4^{3-} in the fluid samples of WV-7 as compared to LM-2 and MIP-3H
24
25 are likely due to the higher dissolution of F and PO_4^{3-} rich minerals present in WV-7 shale
26
27 sample as indicated by their lower saturation index values (Table. 5). Geochemical equilibrium
28
29 modeling showed that both LM-2 and MIP-3H fluids are supersaturated with respect to FCO_3 -
30
31 apatite and hydroxyapatite, while all three HFF-shale experiments are supersaturated with
32
33 respect to fluorite (Table 5). Similar observations of apatite precipitation are reported on
34
35 Huntersville Chert surfaces when exposed to Marcellus Shale produced water (Dieterich et al.,
36
37 2016). Formation of these precipitates can clog up the pore spaces during hydraulic fracturing
38
39 operation and thus have implications on well productivity.
40
41
42
43
44
45
46
47

48 To evaluate how representative the experimental fluids from this study are to field-collected
49
50 produced waters from the Marcellus Shale, we compared the composition of our shale-reacted
51
52 fluids with data reported for Marcellus produced waters by the USGS.⁴¹ Experimental values for
53
54 our shale-reacted experiments (LM-2, MIP-3H, and WV-7) fall within the USGS-reported range
55
56
57
58
59
60

1
2
3 of values (Figure 4). Similarities observed with the mineral reactions between this and prior
4 studies, and with reported produced water compositions from the Marcellus Shale, indicate that
5 the organic reactions discussed in the next section are relevant to Marcellus Shale reservoir
6 conditions.
7
8
9
10
11
12

13 ***4.2 Aqueous Organic Chemistry***

14
15
16
17 Differences in organic chemistry between the NR-HFF, HPT-HFF, and experiments
18 containing shale (LM-2, WV-7, and MIP-3H) indicate that the HFF reacts at elevated P,T both in
19 the absence and presence of shale, and that the shale controls the evolution of aqueous organic
20 chemistry in the LM-2, WV-7 and MIP-3H experiments (Table 4, Figure 3).
21
22
23
24
25
26

27 Exposing HFF to elevated pressure and temperature resulted in differences between the total
28 dissolved organic carbon (DOC) concentrations between the shale-free experiments (where DOC
29 represents the non-purgeable organic carbon (NPOC) and organic acids measured in the
30 experimental fluids) and volatile organic compound (VOC) content (Table 4). The DOC
31 increased for the HPT-HFF relative to the NR-HFF and results from reactions involving the HFF
32 additives. The combination of gelling agent and cross linker are applied during hydraulic
33 fracturing to increase the molecular weight of the injected HFF in order to transport proppant.⁴²
34
35
36
37
38
39
40
41
42
43
44
45
46
47
48
49
50
51
52
53
54
55
56
57
58
59
60
The cross linker also may link other components of the fracturing fluid, resulting in larger
organic molecules that are rendered non-purgeable in the HPT-HFF. Boric acid and
ethanolamine were both included in the HFF recipe used for this study, and boric acid is reported
to catalyze multiple organic transformations.⁴³

1
2
3 Increases in organic acid and VOC content in the absence of shale shows that both classes of
4
5 compounds can be produced solely from HFF exposure to reservoir pressure and temperature
6
7 conditions. Although formate and succinate are present in the NR-HFF solution, likely included
8
9 as part of the HFF chemical additives (Table 1), in the HPT-HFF acetate and butyrate are
10
11 measured above the detection limit, formate concentrations double, and succinate decreases
12
13 (Table 4, Figure 3B). Toluene and xylenes are also generated upon exposure of HFF to reservoir
14
15 conditions and are detectable in HPT-HFF (and below the detection limit in NR-HFF) (Table 4,
16
17 Figure 3C). A prior study showed that certain organic additives, such as gelling and friction
18
19 agents, degraded under reservoir conditions and were able to produce lower molecular weight
20
21 organic compounds.¹⁹
22
23
24
25
26

27 The concentration and speciation of dissolved organic constituents differed in experiments
28
29 containing shale (LM-2, WV-7, MIP-3H) relative to the shale-free HFF reacted at elevated P, T
30
31 (HPT-HFF). Experiments containing shale exhibited similarities across shale types for total
32
33 organic acid concentrations. However, these organic acid concentrations were lower along with
34
35 NPOC when compared to the HPT-HFF fluid (Table 4, Figure 3B). The shale OM matrix
36
37 (kerogen) may act as a location for adsorption of the dissolved organic carbon (DOC; organic
38
39 acids + NPOC) compounds onto the surface. More mature shale contains more aromatic
40
41 compounds within its OM, resulting in higher organic porosity and the relatively high surface
42
43 area within this matrix.^{44,45} This organic porosity creates an effective adsorbent trap for organic
44
45 molecules used or generated in the hydraulic fracturing process.⁴⁵ Other laboratory fluid-shale
46
47 studies observed a similar decrease in DOC in the fluid samples from autoclave reactions, while
48
49 also observing an increase in TOC in the solid sample.^{8,19} Alternatively, components of the shale
50
51 may catalyze the degradation of dissolved OM,^{19,46} subsequently lowering concentrations of
52
53
54
55
56
57
58
59
60

1
2
3 organic acids and NPOC in the LM-2, WV-7, and MIP-3H experiments relative to the HPT-HFF
4
5 experiment.
6
7

8
9 Although organic acid concentrations were lower in the experiments containing shale, it is
10 possible that some of the organic acids released into the fluid were generated from the shale
11 kerogen (as opposed to solely being sourced from the hydraulic fracturing fluid). Low molecular
12 weight carboxylic acids, in particular, acetate and formate, have been observed in both produced
13 water and fluids from similar fluid-shale experiments.^{11,14,47} The proliferation of these
14 compounds is considered to be related to the labile ester linked carboxyl functional groups
15 attached to the OM within the shale formation. These labile functional groups are formed from
16 throughout the process of diagenesis⁴⁸ and are thought to be extracted from the shale reservoir
17 upon hydraulic fracturing and fluid saturation.⁴⁷ Water-soluble organic acids have been measured
18 for separate shale sampled from the MIP-3H well.⁴⁹
19
20
21
22
23
24
25
26
27
28
29
30
31
32

33 Measured VOCs in the LM-2 experiment were the highest out of all fluids sampled (Table 4,
34 Figure 3A). VOCs were higher in both LM-2 and WV-7 compared to the HPT-HFF, and below
35 the detection limit in the MIP-3H experiment (Table 4, Figure 3A). The LM-2 sample contains a
36 larger portion of labile hydrocarbons, as the OM within the shale has not been thermally
37 degraded or altered to the same extent as the high maturity rocks²¹ (LM-2 samples represented as
38 sample BG-1 LM in ²¹). Similar to the degradation of gelling agents, the labile portion of the
39 organic macromolecules in shale are subsequently transformed and solubilized into the fluid
40 under high pressure and temperatures as a result of kerogen reaction.²⁵ It has been shown the
41 persulfate breakers have been utilized to dissolve or breakdown the kerogen within subterranean
42 formations (US Patent 2017/066959A1). Products of oxidizing breakers, such as ammonium
43
44
45
46
47
48
49
50
51
52
53
54
55
56
57
58
59
60

1
2
3 persulfate, have been observed in produced water (e.g., NH_4^+ ; ⁵⁰). These residual breakers might
4
5 react with OM (kerogen) (e.g., ²⁵) and may potentially release these labile compounds over the
6
7 life of the well. The absence of target VOCs in fluid from the MIP-3H experiment is likely a
8
9 result of surface adsorption of VOCs to highly-aromatic kerogen nanopores in the thermally-
10
11 mature shale.^{24,51,52} The relatively high salinity of produced fluid caused by the mixing of
12
13 injection and formation fluid may increase the sorption of organic compounds onto activated
14
15 carbon,⁵³ which may be a proxy for the highly mature kerogen of MIP-3H.
16
17
18
19

20
21 The physical characteristics of the shale OM at the molecular level is a contributing factor in
22
23 the organic composition of produced waters from hydraulically-fractured shale reservoirs and
24
25 should be taken into consideration when assessing environmental impact and recycling strategies
26
27 associated with flowback and produced water. VOCs are commonly observed in both gaseous
28
29 and solubilized forms around hydraulic fracturing operations and fluid-shale experiments.^{3,8,54}
30
31 Separators are effective for reducing some of the VOCs in produced fluid, but some compounds
32
33 remain in the fluids after separator treatment,⁵³ further demonstrating the necessity of knowing
34
35 the source of these compounds over the life of the well.
36
37
38
39

40 **5.0 Conclusions**

41
42
43 Experiments were conducted to understand the inorganic and organic changes that occur in
44
45 fracturing fluid and rock during the shut-in phase of HF operations. Experiments were carried
46
47 out in high P-T autoclave reactors using samples of varying maturity and mineralogy from the
48
49 Marcellus Shale. Our results indicate an increase of SO_4^{2-} and PO_4^{3-} ions and a decrease in
50
51 Ba^{2+} ions in all shale- fluid reactions. The concentrations of these ions are controlled primarily
52
53 by variations in shale mineralogy, especially by its carbonate and clay content. We also observed
54
55
56
57
58
59
60

1
2
3 a net decrease in DOC (organic acids + NPOC) concentrations for all the shale-fluid reactions as
4 compared to control HPT-HFF fluid. Further, we noted a decrease in concentrations of VOCs
5 (benzene, toluene, and xylene) with increasing maturity indicating absorption of these organic
6 species in shale OM.
7
8
9
10
11
12

13 The variations in chemical signatures of reacted fluids clearly suggest that the mineralogy
14 and nature of OM plays a key role in the mobilization of inorganic and organic components
15 during HF operations. It also suggests these reactions can vary significantly in different parts of
16 the basin. Therefore, the chemical composition of HFF's should be modified to better target the
17 varying mineralogical compositions and nature of OM encountered in different parts of the basin.
18 Further investigation on the sorption, transformation, transport, and fate of low molecular weight
19 organic components in fluid-shale reactions is necessary to improve understanding of
20 geochemical reactions during hydraulic fracturing to optimize gas production, minimize
21 environmental impact, and design water reuse and recycling strategies.
22
23
24
25
26
27
28
29
30
31
32
33
34

35 **Acknowledgments**

36
37
38 Samples for this research were provided by SWN energy and the Marcellus Shale Energy and
39 Environment Laboratory (MSEEL) funded by the Department of Energy's National Energy
40 Technology Laboratory (DOE-NETL) grant DE# FE0024297. The research was also funded by
41 Department of Energy's National Energy Technology Laboratory grant DEFE0004000, a
42 National Science Foundation grant (NSF DEB-1342732) to S. Sharma and the Department of
43 Energy's Office of Oil and Natural Gas Unconventional Resources Research Program support of
44 the NETL Research and Innovation Center's Onshore Unconventional Resources Portfolio.
45
46
47
48
49
50
51
52
53
54
55
56
57
58
59
60

FIGURES

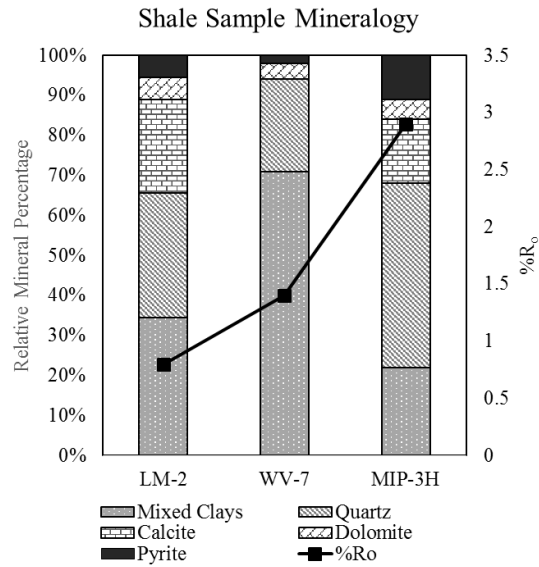


Figure 1. Relative percentages of minerals in three shale samples overlay by their %R_o (maturity) values.

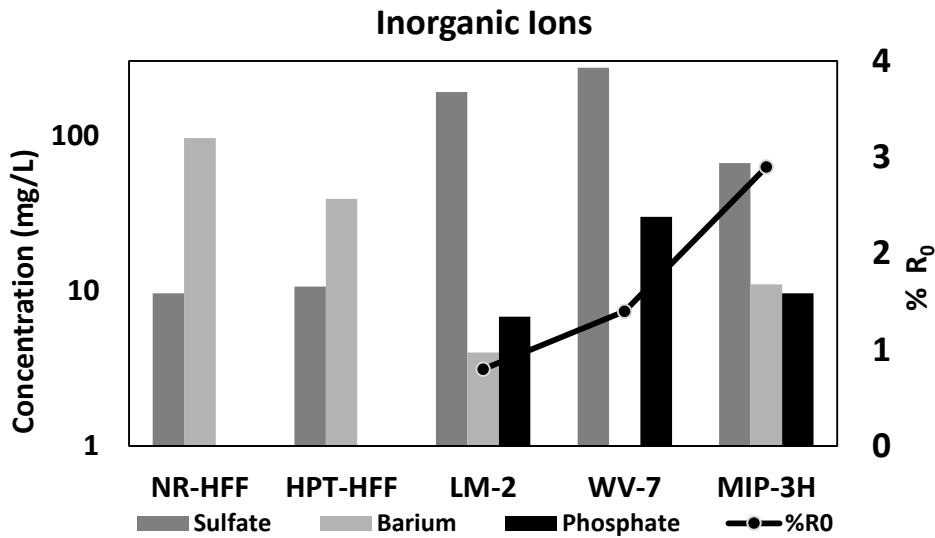
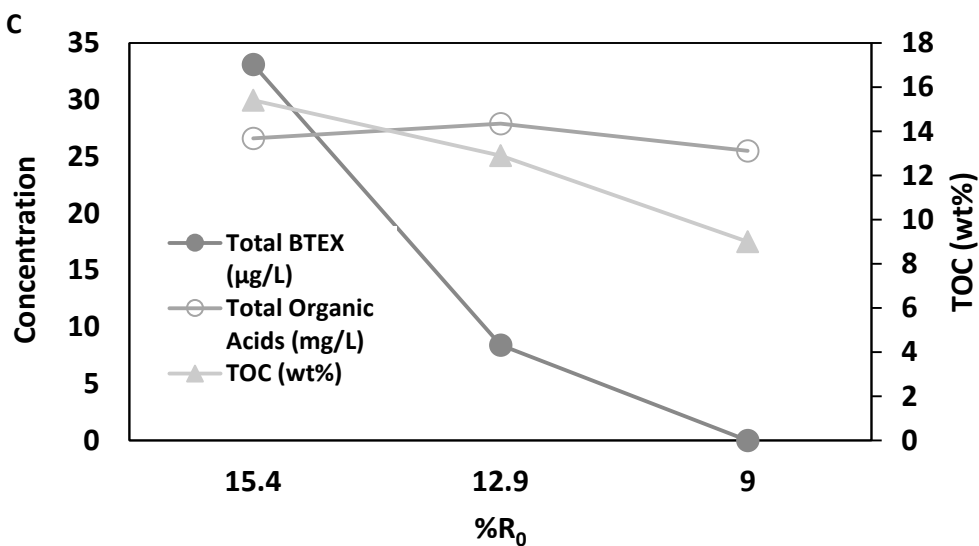
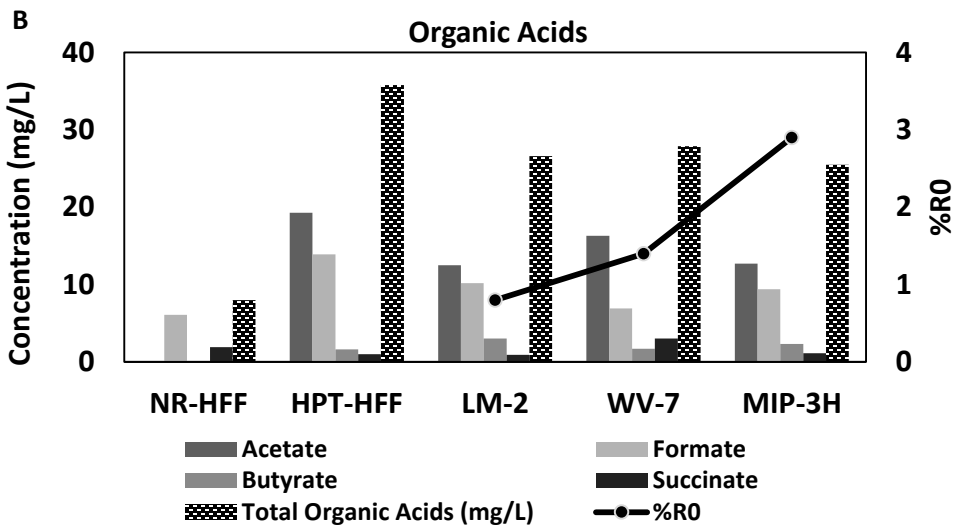
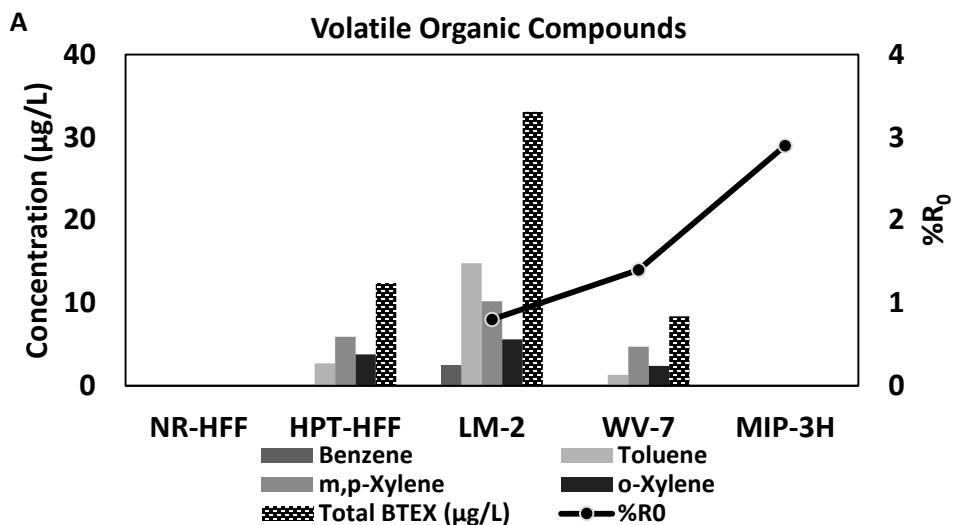
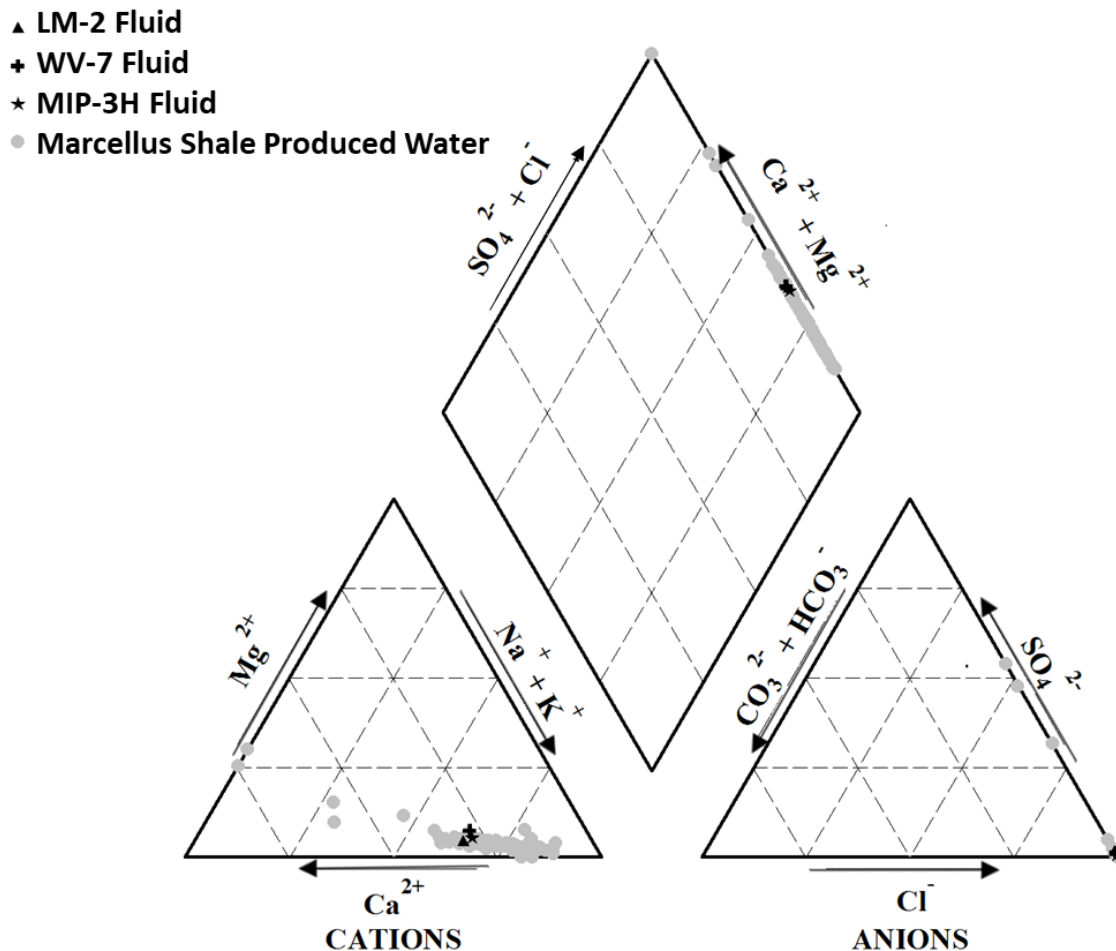


Figure 2. Inorganic ions sulfate (SO₄²⁻), Barium (Ba²⁺), Phosphate (PO₄⁻³) concentrations in all fluid samples plotted with the thermal maturity of the reacted shale.



1
2
3 **Figure 3.** A) Volatile organic compound concentrations in all fluid samples plotted with the
4 thermal maturity for the reacted shales. B) Organic acid concentrations in all fluid samples
5 plotted with the thermal maturity for the reacted shales. C) Plot of the relationship between total
6 targeted VOC's, total targeted organic acids, TOC, and %R₀. For panels A and B, the cross-
7 hatched bar represents the sum of concentrations for each class of compounds measured in the
8 sample. Components without bar display are not detectable (A, B). In panel C, lines are
9 presented to display the direction of the data trend and do not represent a calculated fit of the
10 data.
11
12
13
14
15



46 **Figure 4.** Piper diagram showing the relative amounts of the most abundant ions in
47 solution. Grey dots represent produced water from hydraulic fracturing operations in the
48 Marcellus Shale basin collected by the USGS and the black markers overlain, represent
49 the three fluid samples from fluid-shale reactions in this study.
50
51
52
53
54
55
56
57
58
59
60

Table 1. The chemical composition of the synthetic HFF and brine mixture used for experiments in this study (reproduced from Vankeuren et al., 2017).

Ingredient	Purpose	Concentration	Ingredient	Concentration
		Weight %		Weight %
Deionized Water	Carrier fluid	99.36%	Deionized Water	97.12%
Hydrochloric acid	Perforation cleaner	0.25%	Boric Acid	0.002%
WGA-15L	Gelling agent	0.15%	Potassium Carbonate	0.024%
WCS-631LC	Clay stabilizer	0.106%	Barium Chloride Dehydrate	0.046%
WFR-61LA	Friction reducer	0.049%	Potassium Chloride	0.022%
Ammonium persulfate	Breaker	0.020%	Strontium Chloride Sesquihydrate	0.14%
Glutaraldehyde	Biocide	0.019%	Ammonium Chloride	0.016%
Potassium hydroxide	pH adjuster	0.014%	Sodium Bromide	0.018%
Potassium carbonate	pH adjuster	0.012%	Calcium Chloride Dehydrate	0.74%
Ethylene glycol	Scale Inhibitor	0.0045%	Magnesium Chloride Sesquihydrate	0.19%
Citric acid	Iron control	0.0034%	Sodium Chloride	1.67%
Boric acid	Cross linker	0.0020%	Sodium Sulfate	0.0002%
Ethanolamine	Cross linker	0.0014%	Sodium Bicarbonate	0.015%
WAI-251LC	Corrosion inhibitor	0.0013%		

Composition of Brine

Composition of Hydraulic Fracturing Fluid (HFF)

Table 2. Organic and mineral composition of three shale samples form Marcellus Shale cores, collected from three different depths and geographical areas. The %R₀ and TOC values were reported by (Agrawal and Sharma, 2018b, c). Semi-quantitative XRD data are used for LM-2, WV-7, MIP-3H samples analyzed in this study.

Sample ID	Depth (ft.)	%R ₀	T _{max} (°C)	TOC (wt%)	Quartz (wt%)	Calcite (wt%)	Dolomite (wt%)	Pyrite (wt%)	Mixed Clays (wt%)
LM-2	5825.7	0.8	443	15.4	28	21	5	5	42
WV-7	6615.8	1.4	475	12.9	23	ND	4	2	71
MIP-3H	7511.8	2.9	561	9.0	46	16	5	11	22

Table 3. Cation and anion concentrations in fluid samples in mg/L measured via IC. Also included is pH for each fluid sample and overall total dissolved solids (TDS in mg/L). For dissolved inorganic carbon (DIC), values are either not-detected (ND) or reported in mg as C/L. The values reported are average of samples run in triplicates and the standard error of all measurements are < ± 3%

	pH	F ⁻	Br ⁻	NO ₃ ⁻	SO ₄ ⁻²	PO ₄ ⁻³	Cl ⁻	Li ⁺	Na ⁺	NH ₄ ⁺	K ⁺	Mg ⁺²	Ca ⁺²	Sr ⁺²	Ba ⁺²	DIC
Det. limit	-	0.04	0.26	0.2	0.5	0.4	0.2	0.04	0.4	0.2	0.2	0.2	0.4	0.1	0.1	0.5
NR-HFF	1.3	0.6	107	4.5	9.6	ND	16729	ND	6583	89	393	213	2015	464	96	ND
HPT-HFF	1.9	0.5	60	2.3	10.6	ND	7809	ND	3277	52	165	104	967	224	39	ND
LM-2	6.1	3.2	68	1.7	189.8	6.8	9060	0.1	3727	51	205	132	1606	211	4	35.2
WV-7	2.3	9.9	110	5.1	271.5	29.8	16867	0.2	6663	92	427	418	2576	367	ND	ND
MIP-3H	5.7	3.6	65	1.6	66.1	9.6	8894	0.2	3673	50	202	165	1418	228	11	15.8

Table 4. Dissolved organic carbon (DOC) concentrations in fluid samples in unit of mg/L, where NPOC = non-purgeable organic carbon in unit of mg as C/L, and volatile organic carbon (VOC) concentrations in µg/L, for each fluid sample. The values reported are average of samples run in triplicates and within 2% precision (%RSD).

SAMPLE ID	DOC CONCENTRATIONS IN MG/L					VOC CONCENTRATIONS IN µG/L			
	NPOC	Acetate	Formate	Butyrate	Succinate	Benzene	Toluene	m,p-Xylene	o-Xylene
Det. limit	1.0	0.1	0.1	0.18	0.1	1.0	1.0	2.0	1.0
NR-HFF	243	ND	6.1	ND	1.9	ND	ND	ND	ND
HPT-HFF	317	19.3	13.9	1.6	1.0	0.0	2.7	5.9	3.8
LM-2	264	12.5	10.2	3.0	0.9	2.5	14.8	10.2	5.6
WV-7	197	16.3	6.9	1.7	3.0	ND	1.3	4.7	2.4
MIP-3H	235	12.7	9.4	2.3	1.1	ND	ND	ND	ND

Table 5. Saturation indices for major and potential scale-forming minerals, as calculated in Geochemists Workbench v. 10.0 using the MINTEQ database. Values are reported as log Q/K. Iron- and silica-bearing phases are not included as Fe and Si were not measured in fluids in this study. Blank values indicate that the mineral SI contained no value for that particular calculation.

MINERAL	CHEMICAL FORMULA	NR-HFF	HPT-HFF	LM-2	WV-7	MIP-3H
Barite	BaSO ₄	1.09	1.06	1.35		1.34
Celestite	SrSO ₄	-1.43	-1.37	-0.12	0.11	-0.53
Gypsum	CaSO ₄ ·2H ₂ O	-2.52	-2.44	-0.95	-0.77	-1.44
Calcite	CaCO ₃			-0.82		-1.86
Strontianite	SrCO ₃			-1.22		-2.17
Witherite	BaCO ₃			-3.81		-4.36
FCO₃-Apatite	Ca ₁₀ (PO ₄) ₅ (CO ₃)F ₃			18.77		14.62
Fluorite	CaF ₂	-3.69	-3.01	0.88	0.63	0.93
Hydroxyapatite	Ca ₅ (PO ₄) ₃ (OH)			4.50	-19.41	2.21

REFERENCES

- 1 U.S. EIA, 2017, 14.
- 2 PA DEP, Hydraulic Fracturing Overview,
3 <http://files.dep.state.pa.us/OilGas/BOGM/BOGMPortalFiles/MarcellusShale/DEP%20Fracing%20overview.pdf>.
- 4 S. J. Maguire-Boyle and A. R. Barron, *Environ. Sci. Process. Impacts*, 2014, **16**, 2237–2248.
- 5 A. N. Paukert Vankeuren, J. A. Hakala, K. Jarvis and J. E. Moore, *Environ. Sci. Technol.*, 2017,
6 **51**, 9391–9402.
- 7 A. L. Harrison, A. D. Jew, M. K. Dustin, D. L. Thomas, C. M. Joe-Wong, J. R. Bargar, N.
8 Johnson, G. E. Brown and K. Maher, *Appl. Geochem.*, 2017, **82**, 47–62.
- 9 A. D. Jew, M. K. Dustin, A. L. Harrison, C. M. Joe-Wong, D. L. Thomas, K. Maher, G. E.
10 Brown and J. R. Bargar, *Energy Fuels*, 2017, **31**, 3643–3658.
- 11 Q. Li, A. D. Jew, A. M. Kiss, A. Kohli, A. Alalli, A. R. Kavscek, M. D. Zoback, D. Cercone,
12 K. Maher, G. E. J. Brown and J. R. Bargar, Unconventional Resources Technology Conference,
13 2018.
- 14 V. Marcon, C. Joseph, K. E. Carter, S. W. Hedges, C. L. Lopano, G. D. Guthrie and J. A. Hakala,
15 *Appl. Geochem.*, 2017, **76**, 36–50.
- 16 T. T. Phan, A. N. Paukert Vankeuren and J. A. Hakala, *Int. J. Coal Geol.*, 2018, **191**, 95–111.
- 17 Strong Lisa C., Gould Trevor, Kasinkas Lisa, Sadowsky Michael J., Aksan Alptekin and
18 Wackett Lawrence P., *J. Environ. Eng.*, 2014, **140**, B4013001.
- 19 K. Hoelzer, A. J. Sumner, O. Karatum, R. K. Nelson, B. D. Drollette, M. P. O’Connor, E. L.
20 D’Ambro, G. J. Getzinger, P. L. Ferguson, C. M. Reddy, M. Elsner and D. L. Plata, *Environ.*
21 *Sci. Technol.*, 2016, **50**, 8036–8048.
- 22 B. Ouyang, D. J. Renock, M. A. Ajemigbitse, K. V. Sice, N. R. Warner, J. D. Landis and X.
23 Feng, *Environ. Sci. Process. Impacts*, , DOI:10.1039/C8EM00311D.
- 24 M. A. Ajemigbitse, F. S. Cannon, M. S. Klima, J. C. Furness, C. Wunz and N. R. Warner,
25 *Environ. Sci. Process. Impacts*, , DOI:10.1039/C8EM00248G.
- 26 K. Lee and J. Neff, Eds., *Produced Water: Environmental Risks and Advances in Mitigation*
27 *Technologies*, Springer-Verlag, New York, 2011.
- 28 M. Elsner and K. Hoelzer, *Environ. Sci. Technol.*, 2016, **50**, 3290–3314.
- 29 A. J. Sumner and D. L. Plata, *Environ. Sci. Process. Impacts*, 2018, **20**, 318–331.
- 30 N. Abualfaraj, P. L. Gurian and M. S. Olson, *Environ. Eng. Sci.*, 2014, **31**, 514–524.
- 31 FracFocus Chemical Disclosure Registry, <http://fracfocus.org/>, (accessed 15 February 2019).
- 32 T. L. Tasker, P. K. Piotrowski, F. L. Dorman and W. D. Burgos, *Environ. Eng. Sci.*, 2016, **33**,
33 753–765.
- 34 V. Agrawal and S. Sharma, *Front. Energy Res.*, , DOI:10.3389/fenrg.2018.00042.
- 35 V. Agrawal and S. Sharma, *Fuel*, , DOI:<https://doi.org/10.1016/j.fuel.2018.04.053>.
- 36 V. Agrawal, Ph.D., West Virginia University, 2018.
- 37 V. Agrawal and S. Sharma, *Sci. Rep.*, 2018, **8**, 17465.
- 38 P. R. Craddock, T. V. Le Doan, K. Bake, M. Polyakov, A. M. Charsky and A. E. Pomerantz,
39 *Energy Fuels*, 2015, **29**, 2197–2210.
- 40 M. K. Dustin, J. R. Bargar, A. D. Jew, A. L. Harrison, C. Joe-Wong, D. L. Thomas, G. E. Brown
41 and K. Maher, *Energy Fuels*, 2018, **32**, 8966–8977.
- 42 R. Chen, S. Sharma, T. Bank, D. Soeder and H. Eastman, *Appl. Geochem.*, 2015, **60**, 59–71.
- 43 D. . Jarvie and L. . Lundell, The Woodlands, Texas, 1991.

- 1
2
3 28F. H. Chung, *J. Appl. Crystallogr.*, 1974, **7**, 519–525.
4 29F. H. Chung, *J. Appl. Crystallogr.*, 1975, **8**, 17–19.
5 30T. R. Malizia, *Geochemistry of the Marcellus Shale; Metals mobility and solubilization*, 2011.
6 31P. Staub, *Clay mineralogy of the Marcellus and Utica Shales: Implications for fluid*
7 *development via cation exchange*, 2014.
8 32D. Knetsch and W. L. Groeneveld, *Inorganica Chim. Acta*, 1973, **7**, 81–87.
9 33J.-Y. Fang and C. Shang, *Environ. Sci. Technol.*, 2012, **46**, 8976–8983.
10 34T. Phan, A. Hakala and D. Bain, *Appl. Geochem.*, 2018, **95**, 85–96.
11 35F. D. H. Wilke, A. Vieth-Hillebrand, R. Naumann, J. Erzinger and B. Horsfield, *Appl.*
12 *Geochem.*, 2015, **63**, 158–168.
13 36M. Dieterich, B. Kutchko and A. Goodman, *Fuel*, 2016, **182**, 227–235.
14 37D. Renock, J. D. Landis and M. Sharma, *Appl. Geochem.*, 2016, **65**, 73–86.
15 38A. D. Jew, Q. Li, D. Cercone, K. Maher, G. E. J. Brown and J. R. Bargar, Unconventional
16 Resources Technology Conference, 2018.
17 39L. Wang, S. Burns, D. E. Giammar and J. D. Fortner, *Chemosphere*, 2016, **149**, 286–293.
18 40J. Yang, M. Torres, J. McManus, T. J. Algeo, J. A. Hakala and C. Verba, *Chem. Geol.*, 2017,
19 **466**, 533–544.
20 41M. . Blondes, K. . Gans, M. . Engle, Y. . Kharaka, M. . Reidy, V. Saraswathula, J. . Thordsen,
21 E. . Rowan and E. . Morrissey, *USGS*.
22 42O. US EPA, Proceedings of the Technical Workshops for the Hydraulic Fracturing Study,
23 [https://www.epa.gov/hfstudy/proceedings-technical-workshops-hydraulic-fracturing-study-](https://www.epa.gov/hfstudy/proceedings-technical-workshops-hydraulic-fracturing-study-chemical-and-analytical-methods)
24 [chemical-and-analytical-methods](https://www.epa.gov/hfstudy/proceedings-technical-workshops-hydraulic-fracturing-study-chemical-and-analytical-methods), (accessed 15 February 2019).
25 43R. Pal, *Arkivoc*, 2018, **2018**, 346–371.
26 44S. Zargari, K. L. Canter and M. Prasad, *Fuel*, 2015, **153**, 110–117.
27 45T. Zhang, G. S. Ellis, S. C. Ruppel, K. Milliken and R. Yang, *Org. Geochem.*, 2012, **47**, 120–
28 131.
29 46B. Xiong, Z. Miller, S. Roman-White, T. Tasker, B. Farina, B. Piechowicz, W. D. Burgos, P.
30 Joshi, L. Zhu, C. A. Gorski, A. L. Zydney and M. Kumar, *Environ. Sci. Technol.*, 2018, **52**,
31 327–336.
32 47Y. Zhu, A. Vieth-Hillebrand, F. D. H. Wilke and B. Horsfield, *Int. J. Coal Geol.*, 2015, **150–**
33 **151**, 265–275.
34 48T. I. Eglinton, C. D. Curtis and S. J. Rowland, *Mineral. Mag.*, 1987, **51**, 495–503.
35 49J. A. Hakala, T. Phan, M. Stuckman, H. Edenborn and C. Lopano, *Unconv. Resour. Technol.*
36 *Conf.*, , DOI:10.15530/URTEC-2017-2670833.
37 50J. S. Harkness, G. S. Dwyer, N. R. Warner, K. M. Parker, W. A. Mitch and A. Vengosh, *Environ.*
38 *Sci. Technol.*, 2015, **49**, 1955–1963.
39 51V. Agrawal and S. Sharma, *Sci. Rep.*, 2019, (in review).
40 52G. Cornelissen, Ö. Gustafsson, T. D. Bucheli, M. T. O. Jonker, A. A. Koelmans and P. C. M.
41 van Noort, *Environ. Sci. Technol.*, 2005, **39**, 6881–6895.
42 53A. Butkovskiy, H. Bruning, S. A. E. Kools, H. H. M. Rijnaarts and A. P. Van Wezel, *Environ.*
43 *Sci. Technol.*, 2017, **51**, 4740–4754.
44 54W. Orem, C. Tatu, M. Varonka, H. Lerch, A. Bates, M. Engle, L. Crosby and J. McIntosh, *Int.*
45 *J. Coal Geol.*, 2014, **126**, 20–31.
46
47
48
49
50
51
52
53
54
55
56
57
58
59
60